

# Preparation of Silver Nanoparticles by Using Tripropylene Glycol as the Reducing Agents of Polyol Process

Tzu Hsuan Chiang, K.-D. Wu, and Tsung-Eong Hsieh

**Abstract**—Silver (Ag) nanoparticles were prepared by the polyol process using tripropylene glycol, 3-ethyl-3-oxetanemethanol, and polycaprolactone triol as the reducing agents and poly(vinylpyrrolidone) (PVP) with average molecular weights ( $M_w$ ) of 10 000, 55 000, and 1 300 000 as the protective agent, respectively. It was found that the sizes of Ag particles were affected by the type of reducing agent,  $M_w$  of PVP, the concentration of PVP, reaction temperature, and time. The Ag nanoparticles as small as 34.4 nm were achieved when the reaction was conducted at atmospheric ambient and a temperature of 120 °C for 3 h by using tripropylene glycol as the reducing agent and 20 wt.% PVP with an  $M_w$  of 55 000. The nanoscale Ag particles with face-centered cubic structure exhibited a strong surface plasmon resonance peak at 350 nm in the UV-visible spectrum.

**Index Terms**—Polyol process, reducing agent, silver nanoparticles, tripropylene glycol.

## I. INTRODUCTION

SILVER nanoparticles have attracted the attention of numerous researchers in the electronic industry due to their high electrical conductivity and because they are an essential component of the conducting inks, pastes, and adhesives that are used for the fabrication of various electrical parts [1]–[3]. Nanoscale Ag powders can be prepared either by physical processes, such as mechanical milling [4], or by chemical processes, such as reduction reactions [5], [6], photochemical or radiation-chemical reduction reactions [7], [8], sonochemical reactions [9], and polyol process [10]. Among these alternatives, the polyol process has been demonstrated to be a reliable method for the synthesis of metallic nanoparticles with high purity and uniform particle size [11]. Fievet *et al.* [11] first utilized ethylene glycol (EG, HOCH<sub>2</sub>-CH<sub>2</sub>OH) as the reducing agent and solvent for the reduction of silver nitrate (AgNO<sub>3</sub>) to yield Ag nanoparticles at 160 °C without using poly(vinylpyrrolidone) (PVP). In

TABLE I  
SUMMARY OF REDUCTION CONDITIONS OF AgNO<sub>3</sub> IN EG WITH PVP [12]–[18]

Reaction temperature (°C)	Time (hr)	Ag particle size	Ref.
186	4	10.4 nm	[12]
186	3	33 nm	[13]
170	1	Nanowire, 30 ~ 60 nm	[13]
120	1.5	Length: 0.5 ~ 1 μm Width: 100 ~ 200 nm	[15]
170	1.5	Nanorod, 2 ~ 5 μm	[16]
120	22	21 nm	[17]
140	1	144 nm	[18]
120	3	34.4 nm	This work

subsequent studies of the synthesis of Ag nanoparticles [12]–[18], PVP was dissolved in EG and the reactions were commonly performed at temperatures ranging from 120 to 186 °C (see Table I). Alternatively, He *et al.* [19] studied the usage of methanol (CH<sub>3</sub>OH), 2-propanol ((CH<sub>3</sub>)<sub>2</sub>CHOH), ethanol (C<sub>2</sub>H<sub>5</sub>OH), and N, N-dimethylformamide (DMF, (CH<sub>3</sub>)<sub>2</sub>NCOH) as the reducing agents in the polyol process. These reducing agents contain hydroxyl groups (–OH) groups that can react with AgNO<sub>3</sub> during the reduction reaction. The utilization of several other types of reducing agents has been reported, including poly(ethylene glycol) (C<sub>2n+2</sub>H<sub>4n+6</sub>O<sub>n+2</sub>) [20]–[22], glycerol (C<sub>3</sub>H<sub>5</sub>(OH)<sub>3</sub>) [23], glycolaldehyde (C<sub>2</sub>H<sub>4</sub>O<sub>2</sub>) [24], sugars [25], sodium citrates [26], and NaBH<sub>4</sub> [27].

This study investigates the synthesis of Ag nanoparticles using monomers that contain –OH groups as the reducing agents [28], e.g., tripropylene glycol (H(OC<sub>3</sub>H<sub>6</sub>)<sub>3</sub>OH), 3-ethyl-3-oxetanemethanol (C<sub>6</sub>H<sub>12</sub>O<sub>2</sub>), and polycaprolactone triol (C<sub>2</sub>H<sub>5</sub>C[CH<sub>2</sub>O[CO(CH<sub>2</sub>)<sub>5</sub>O]<sub>n</sub>H]<sub>3</sub>), and using PVP as the protecting agent in order to control the size of the Ag particles. Fig. 1 shows the chemical structures of the reducing agents that were used. The effects of the reducing agent types, average molecular weight ( $M_w$ ) and concentration of PVP, reaction temperatures and reaction times on the sizes, shapes, and morphologies of the Ag nanoparticles were characterized, and relevant discussions are presented in the following sections.

Manuscript received May 23, 2013; revised August 26, 2013; accepted November 19, 2013. Date of publication December 12, 2013; date of current version January 6, 2014. This work was supported in part by the National Science Council, Taiwan, R.O.C., under the contract no. NSC100-2221-E-009-055-MY3. The review of this paper was arranged by Associate Editor L. Dong.

T. H. Chiang is with the Department of Energy Engineering, National United University, Miaoli, Taiwan 36003, R.O.C. (e-mail: thchiang@nuu.edu.tw).

K.-D. Wu and T.-E. Hsieh are with the Department of Materials Science and Engineering, National Chiao Tung University, Hsinchu, Taiwan 30010, R.O.C. (e-mail: kdwu@yahoo.com.tw; tehsieh@mail.nctu.edu.tw).

Color versions of one or more of the figures in this paper are available online at <http://ieeexplore.ieee.org>.

Digital Object Identifier 10.1109/TNANO.2013.2294174

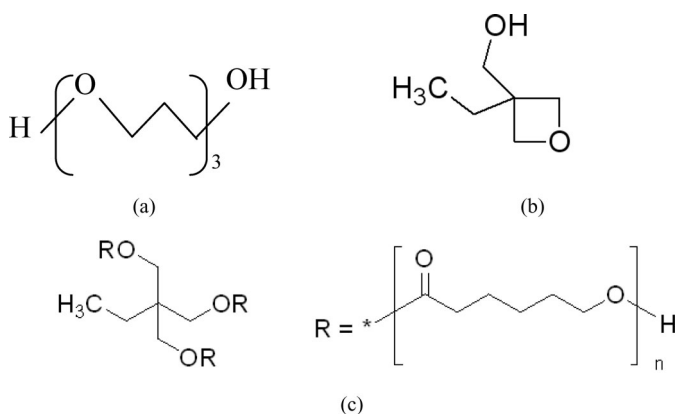


Fig. 1. Chemical structures of (a) tripropylene glycol, (b) 3-ethyl-3-oxetanemethanol, and (c) polycaprolactone triol.

## II. EXPERIMENTAL

### A. Materials

The  $\text{AgNO}_3$  was supplied by HWANG LONG, Ltd., Taiwan. Tripropylene glycol, 3-ethyl-3-oxetanemethanol, polycaprolactone triol, and PVP with  $M_w$  of 10 000, 55 000, and 1 300 000, respectively, were purchased from the Aldrich Company.

### B. Preparation of Ag Nanoparticles

First, at room temperature, various amounts of PVP were dissolved separately in the three types of reducing agents as listed below. PVP with  $M_w = 10\ 000$ : solutions containing 10, 15, and 20 wt.% of PVP were prepared. PVP with  $M_w = 55\ 000$ : solutions containing 2, 10, 15, and 20 wt.% of PVP were prepared. PVP with  $M_w = 1\ 300\ 000$ : solution containing 10 wt.% of PVP were prepared. Then, appropriate amounts of  $\text{AgNO}_3$  were added to the above mixtures at the fixed weight ratio of  $\text{AgNO}_3$ :reducing agent = 1:100. All of the solutions were heated to  $120\ ^\circ\text{C}$  at a heating rate of  $4\ ^\circ\text{C}/\text{min}$ , and the reduction reaction was allowed to proceed at this temperature for 3 or 24 h. By adding the alcohol solution and oscillating the mixture in an ultrasonic cleaner for 10 min, the Ag nanoparticles were extracted from the reaction products *via* centrifugation (EBA21, Hettich). The cleaning procedures for above products were repeated for at least five times to remove the residual reducing agents and PVP.

### C. Microstructure Characterizations

1) *X-Ray Diffraction*: Appropriate amounts of the Ag nanoparticles were mounted on  $1\ \text{cm} \times 1\ \text{cm}$  glass plates and then transferred to an *x*-ray diffractometer (XRD, MacScience M18XHF) to characterize the structure of nanoparticles. The *x*-ray light source was  $\text{Cu-K}\alpha$  radiation with a wavelength of 0.154 nm. The data scanning rate was  $5^\circ/\text{min}$  for diffraction angles ranging from  $30^\circ$  to  $90^\circ$ .

2) *UV-Visible Spectroscopy*: The absorption spectra of the alcohol solutions containing Ag nanoparticles were obtained by a Hitachi U-2001 UV-visible spectrometer equipped with a 10-mm quartz cell. Solution samples for UV-visible

spectroscopic analysis were prepared by adding 0.1 g of the Ag nanoparticle mixture to 10 mL of alcohol.

3) *Fourier-Transform Infrared (FT-IR) Spectroscopy*: For FT-IR analysis, the alcohol solutions that contained the Ag nanoparticles were spin coated on KBr discs. The analysis was achieved by using a PerkinElmer Spectrum 100 FT-IR spectrometer in the wavenumber range of  $400\text{--}4000\ \text{cm}^{-1}$  and the spectral resolution of  $4\ \text{cm}^{-1}$ .

4) *Nuclear Magnetic Resonance (NMR) Analysis*: The samples for NMR analysis were prepared by adding the Ag nanoparticles to the  $\text{CDCl}_3$  solution. The  $^{13}\text{C}$ -NMR spectra of the samples were obtained by using a VARIAN 300 MHz NMR spectrometer.

5) *Transmission Electron Microscopy (TEM)*: The alcohol solutions that contained the Ag nanoparticles were oscillated in an ultrasonic cleaner for 30 min to form uniformly dispersed solutions. Afterward the solutions were dispensed on carbon-clad Cu mesh and dried at  $90\ ^\circ\text{C}$  to complete the sample preparation for TEM characterization. The morphologies of the Ag nanoparticles were characterized by a Philips TECNAI 20 TEM equipped with energy dispersive spectroscopy (EDS, Genesis) and operated at an accelerating voltage of 200 kV. TEM micrographs also were used to calculate the sizes of the Ag nanoparticles with the aid of ImagePro 5.0 analytical software (Media Cybernetics, Inc).

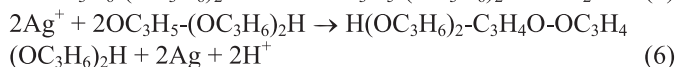
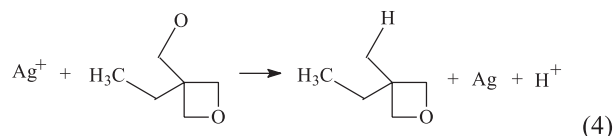
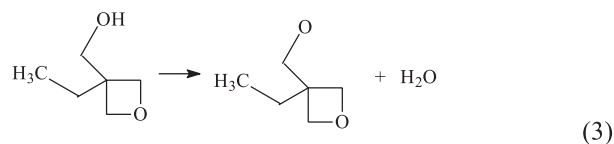
## III. RESULTS AND DISCUSSION

### A. Effects of Reducing Agent Types

According to the polyol reduction mechanism proposed by Fievet *et al.* [11], the metal (M) is formed by the reduction of  $\text{M}^+$  ions *via* the reactions shown as follows:



Accordingly, the reduction reactions initiated by 3-ethyl-3-oxetanemethanol can be expressed by (3) and (4), while the reactions initiated by tripropylene glycol can be expressed by (5) and (6). Note that hydrogen ions ( $\text{H}^+$ ) are produced by the reduction of an  $\text{Ag}^+$  ion to a metallic Ag [29], as indicated by (4) and (6) as follows:



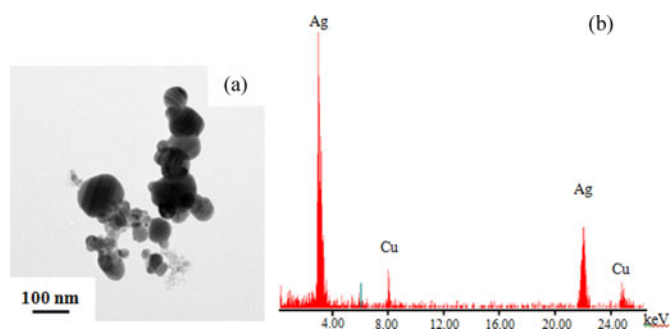


Fig. 2. (a) TEM micrograph and (b) EDS profile of Ag nanoparticles obtained by using 3-ethyl-3-oxetanemethanol as the reducing agent at reaction temperatures of 120 °C for 3 h without adding PVP.

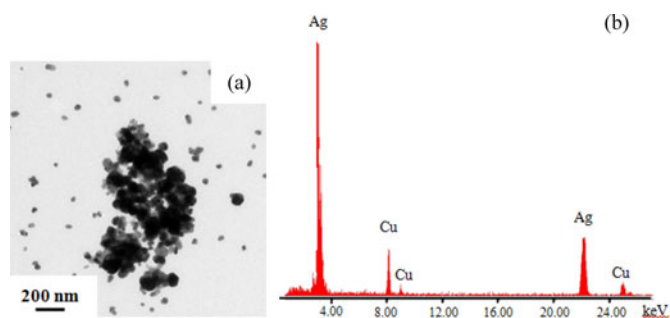


Fig. 3. (a) TEM micrograph and (b) EDS profile of Ag nanoparticles obtained by using tripropylene glycol as the reducing agent at reaction temperatures of 120 °C for 3 h without adding PVP.

Figs. 2(a) and 3(a) present the TEM micrographs of the Ag nanoparticles prepared by using 3-ethyl-3-oxetanemethanol and tripropylene glycol, respectively, as the reducing agents at the reaction temperature of 120 °C for 3 h without adding PVP. The formation of the Ag phase was identified by EDS, as shown in Figs. 2(b) and 3(b). Note that the Cu signals in the EDS profiles are originated from the Cu mesh used for the TEM sample preparation. Moreover, no Ag phase was detected when polycaprolactone triol was used as the reducing agent in the polyol process, indicating that the –OR groups on polycaprolactone triol could not initiate the reduction reaction. A comparison of Figs. 2(a) and 3(a) indicates that the utilization of tripropylene glycol resulted in smaller Ag nanoparticles than those obtained by using 3-ethyl-3-oxetanemethanol. Tripropylene glycol contains three –OH groups, while 3-ethyl-3-oxetanemethanol has only one, and the greater number of –OH group on the tripropylene glycol molecules might cause the acceleration of reactivity, leading to the efficient formation of the aldehyde group compound during the reaction. The aldehyde group compound might promote the formation of Ag nuclei, thereby producing smaller Ag nanoparticles and increasing product yield at the same reaction time.

Fig. 4 presents a representative XRD pattern of the Ag nanoparticles produced by using tripropylene glycol as the reducing agent. The Ag nanoparticles with face-centered-cubic (FCC) structure can be identified according to Joint Committee of Powder Diffraction Standard No. 26–0339.

FT-IR spectra of pure tripropylene glycol and the hybrid of tripropylene glycol and  $\text{AgNO}_3$  are presented in Fig. 5. The peaks at 1650 and 1720  $\text{cm}^{-1}$  correspond to the vibration of the –C–O

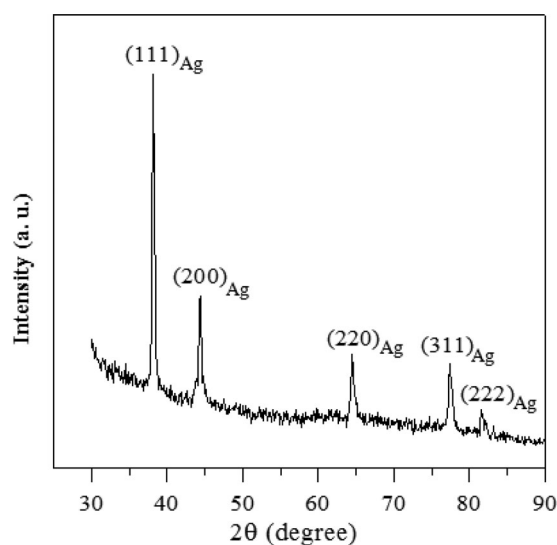


Fig. 4. XRD pattern of Ag nanoparticles obtained by using tripropylene glycol as the reducing agent.

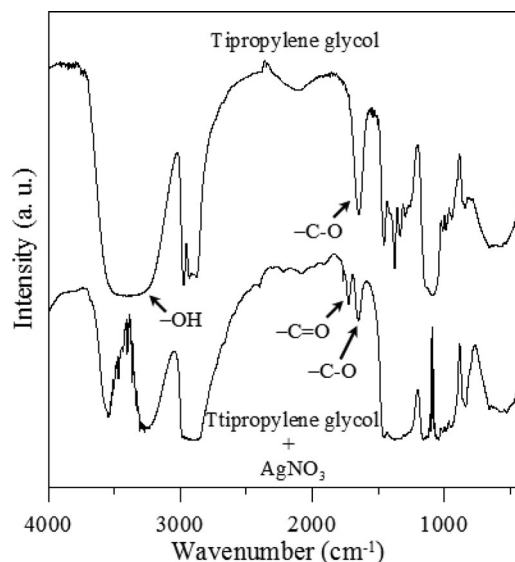


Fig. 5. FTIR spectra of pure tripropylene glycol and hybrid of tripropylene glycol and  $\text{AgNO}_3$ .

bond of tripropylene glycol and of the ketone (–C = O) on the aldehyde group, respectively, illustrating the presence of the intermediate,  $\text{OC}_3\text{H}_5-(\text{OC}_3\text{H}_6)_2$ , during the reduction reaction. This is further evidenced by the peak in the  $^{13}\text{C}$ -NMR spectra at 207.12 ppm (see Fig. 6), which indicates the formation of an intermediate, i.e., a ketone on an aldehyde group, during the reduction reaction. The intermediate is the key component that may promote the formation of Ag particles, as depicted by (6).

### B. Effects of Reaction Temperature

Figs. 7(a) and 7(b) separately present the TEM micrographs of the Ag nanoparticles obtained by using tripropylene glycol as the reducing agent at reaction temperatures of 80 and 120 °C for 3 h without adding PVP. It is apparent that the size of Ag particle decreased as the reaction temperature was increased. This resulted from the increasing reduction reactivity of

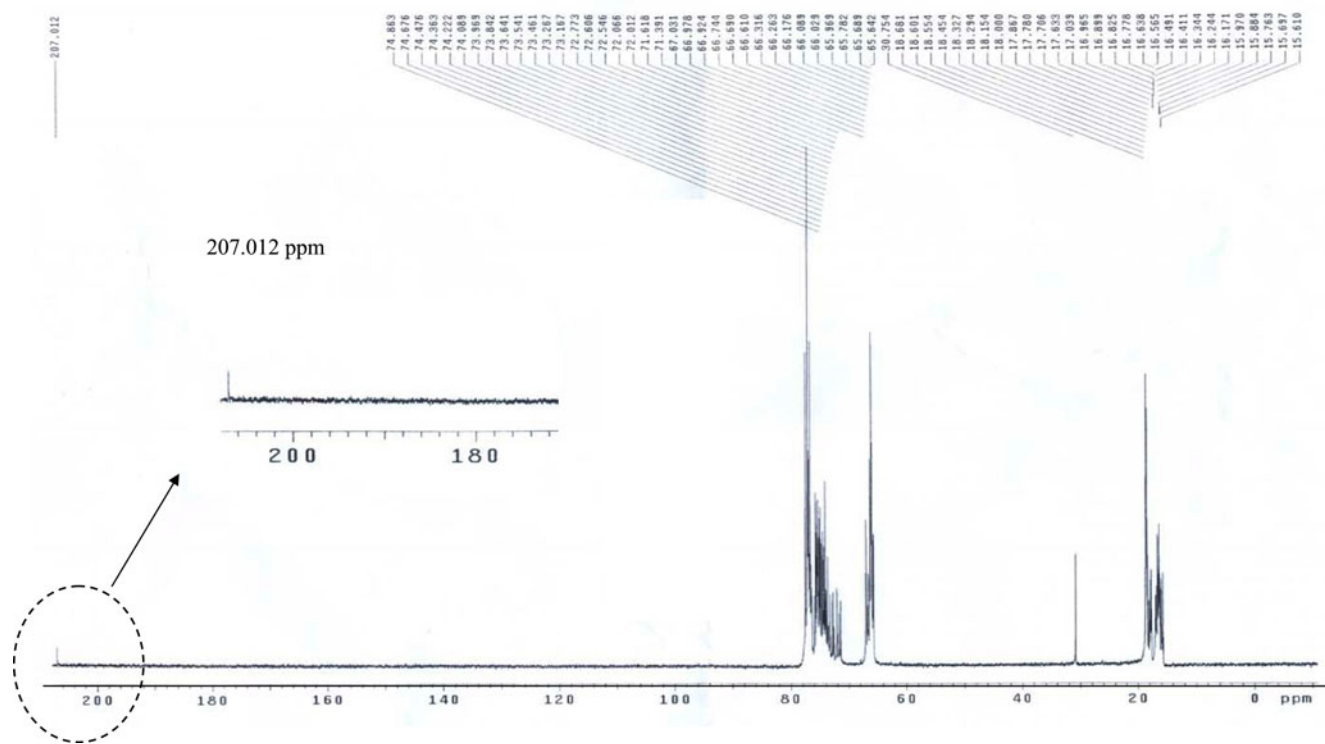


Fig. 6.  $^{13}\text{C}$ -NMR spectra of hybrid of tripropylene glycol and  $\text{AgNO}_3$ .

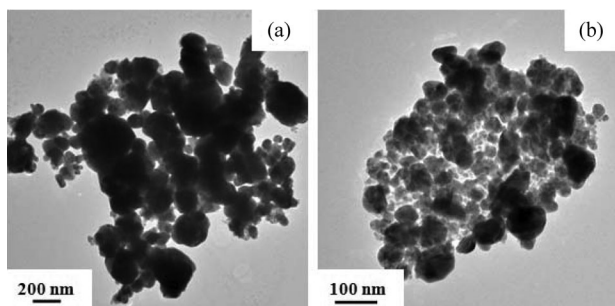


Fig. 7. TEM micrographs of Ag nanoparticles obtained by using tripropylene glycol as the reducing agent at reaction temperature of (a) 80 and (b) 120 °C for 3 h without adding PVP.

tripropylene glycol at higher temperatures, which promoted the formation of Ag nuclei. Usov *et al.* reported similar results, i.e., when sugars was used as the reducing agent, the size of Ag particles decreased when the reaction temperature was increased from 30 to 60 °C [30].

### C. Effects of $M_w$ and Concentration of PVP

It is widely known that adding organic protective agents, such as PVP, to reacting solutions may prevent particle aggregation and control the particle shape [13]. PVP is a homopolymer in which the individual unit contains an amide group. The N and O components in such a polar group have a strong affinity for Ag, which allows the control of the size of Ag particles. All samples discussed in this section were prepared at 120 °C for 3 h by using tripropylene glycol as the reducing agent and PVP as the protecting agent at various  $M_w$  values and weight ratios.

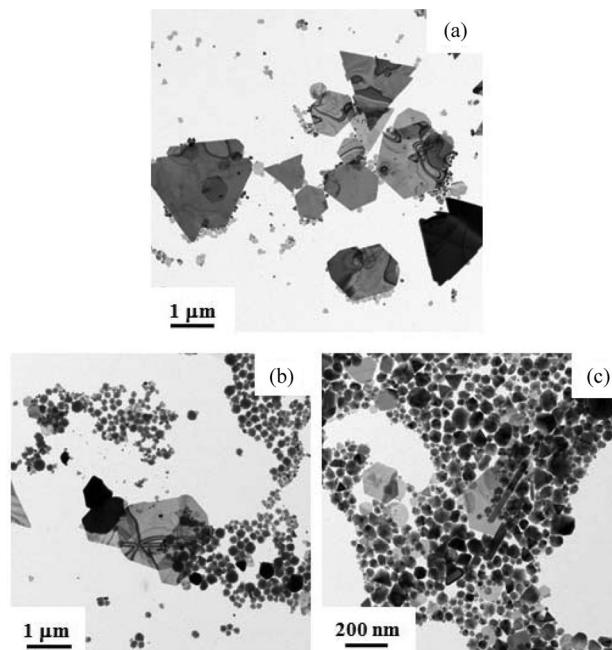


Fig. 8. TEM micrographs of Ag particles prepared at 120 °C for 3 h by using tripropylene glycol as the reducing agent and (a) 10, (b) 15, and (c) 20 wt.% of PVP with an  $M_w$  of 10 000.

Fig. 8(a)–(c) and Fig. 9(a)–(c) show the TEM micrographs of Ag nanoparticles prepared by using PVP with  $M_w = 10\,000$  and 55 000, respectively, at various weight ratios. These figures show that the shape of particles and their degree of aggregation apparently depend on the PVP concentration and PVP's  $M_w$ .



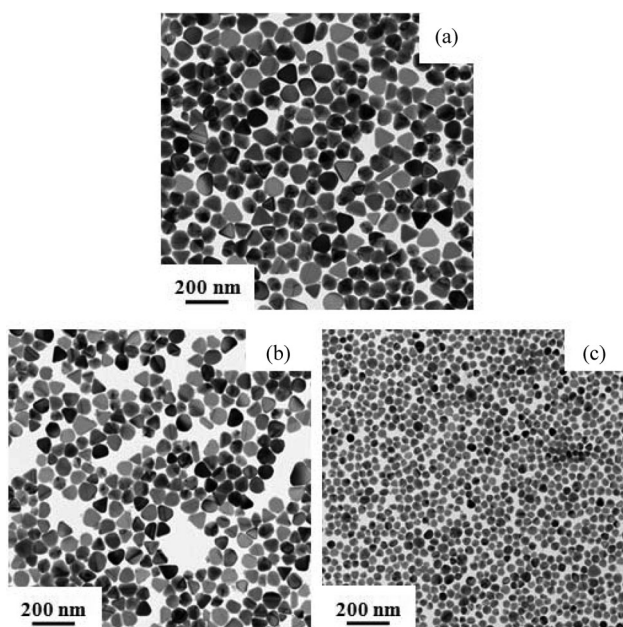


Fig. 9. TEM micrographs of Ag particles prepared at 120 °C for 3 h by using tripropylene glycol as the reducing agent and (a) 10, (b) 15, and (c) 20 wt.% of PVP with an  $M_w$  of 55 000.

Regardless of the value of  $M_w$ , the particle size decreased as the concentration of PVP increased. As shown in Figs. 8(a), large, flake-like Ag particles with polygonal shapes were obtained in the sample that had 10 wt.% PVP with an  $M_w$  of 10 000. Particle refinement occurred when the PVP concentration was equal to or greater than 15 wt.%, as shown in Figs. 8(b) and (c), but flake-like Ag particles also were observed. The results presented in Fig. 8 indicate that low- $M_w$  PVP is insufficient to prevent the coarsening of Ag particles because there were fewer nucleation sites on the shorter polymer chain. While the addition of a relatively large quantity of low- $M_w$  PVP plausibly could produce nanoscale Ag particles, this approach would not result in uniform particle size or shape.

Fig. 9(a)–(c) indicates that the size of the Ag particles decreased dramatically and that the particles became round up when PVP with an  $M_w$  of 55 000 was used. Apparently, the value of  $M_w$  or, the chain length, of the protecting agent was a key factor in controlling the size of Ag particles. Analysis of the images showed that the average size of the Ag particles decreased from 74.1 nm for a PVP concentration of 10 wt.% to 34.4 nm for a PVP concentration of 20 wt.%. Fig. 9 also shows that the uniformity of the shape of the particles increased as the size of particles decreased due to the addition of the protective agent with an appropriate  $M_w$  value. This is illustrated by Fig. 9(c), in which most of the Ag nanoparticles exhibit good sphericity.

Fig. 10 presents the TEM micrograph of the Ag nanoparticles prepared by using PVP with an  $M_w$  of 1 300 000. A comparison of Figs. 9(a) and 10 indicates that, at the same PVP concentration, the sizes of the Ag nanoparticles prepared by using PVP with an  $M_w$  of 1 300 000 are similar to those prepared by using PVP with an  $M_w$  of 55 000. Since PVP with an  $M_w$  of 1 300 000 contains more repeating units per molecule than the PVP with

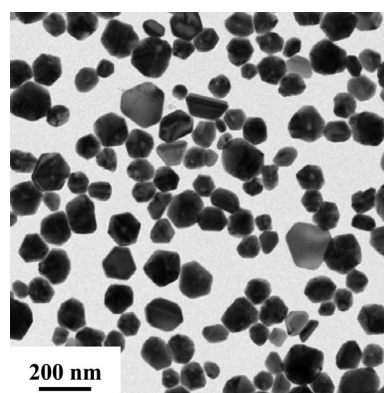


Fig. 10. TEM micrographs of Ag nanoparticles prepared at 120 °C for 3 h by using tripropylene glycol as the reducing agent and 10 wt.% of PVP with an  $M_w$  of 1 300 000.

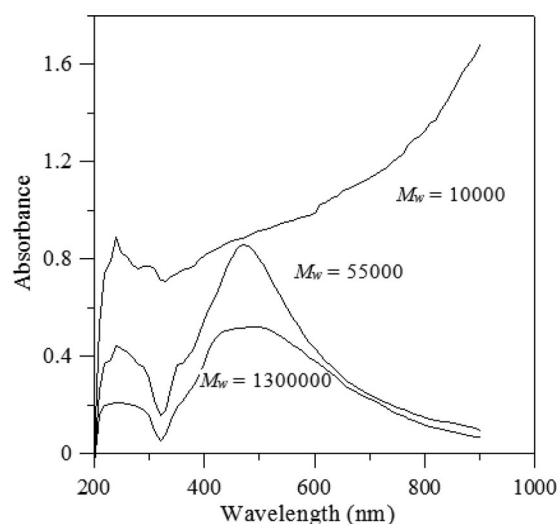


Fig. 11. UV-visible extinction spectra of Ag particles prepared at 120 °C for 3 h by using tripropylene glycol as the reducing agent and PVP with various  $M_w$ 's.

an  $M_w$  of 55 000, it attracts more  $\text{Ag}^+$  ions per molecule and, hence, the Ag nanoparticles are more likely to aggregate as they are growing. Such a result is illustrated by Fig. 11 which presents the UV-visible extinction spectra obtained from solution samples prepared by using 10 wt.% of PVP with various  $M_w$  values. The UV-visible spectroscopy is a useful tool for analyzing the morphological effects and kinetics of nanoparticle formation in terms of the surface plasma resonance (SPR) excitations [31]–[33]. For the samples prepared by using PVP with  $M_w$  values of 55 000 and 1 300 000, the SPR peak at 470 nm indicated the formation of colloidal Ag nanoparticles [34]. In addition, Fig. 11 shows that the bandwidth of the 470 nm peak for the sample prepared by using PVP with an  $M_w$  of 55 000 was slightly wider than that of the sample prepared by using PVP with an  $M_w$  of 1 300 000. The wider bandwidth implies the presence of nanoparticles with smaller sizes [31], in agreement with our TEM calibration, which indicated that the average size of the Ag nanoparticles prepared by using 10 wt.% of PVP with an  $M_w$  of 55 000 was 74.1 nm, while those prepared by using 10 wt.% PVP with an  $M_w$  of 1 300 000 was 81.3 nm. Hence, optimization of the  $M_w$  value of the protecting agent is also a key factor in producing the desired size of the Ag nanoparticles.

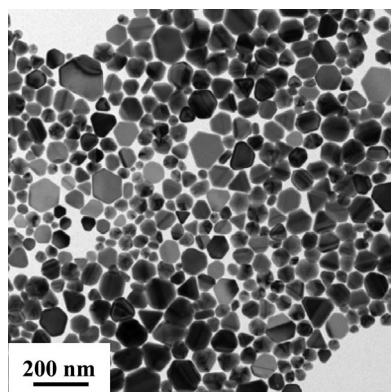


Fig. 12. TEM micrographs of Ag nanoparticles prepared by at 120 °C for 24 h by using tripropylene glycol as the reducing agent and 10 wt.% of PVP with an  $M_w$  of 55 000.

The results presented in Figs. 8 and 9 also indicate that the PVP concentration is another factor affecting the size and shape of the Ag nanoparticles. Regardless of the  $M_w$  value, the particle size decreased as the PVP concentration increased. The evolution of particle size delineated above can be explained in terms of the steric hindrance effect. Low PVP concentration provides insufficient steric hindrance to inhibit the aggregation of Ag particles due to incomplete coverage of the surface of the particles. Thus, a sufficient concentration of PVP is, hence, essential for producing Ag nanoparticles with uniform morphology.

UV-visible spectroscopy can be used to analyze the morphological evolution involved in the growth process because the Ag nanoparticles with different shapes exhibit characteristic SPR bands at different frequencies. Fig. 11 shows that a shoulder peak occurred at about 350 nm for the sample prepared by using PVP with an  $M_w$  of 55 000. Wiley *et al.* [35] reported that cubic-phase nanoparticles possess SPR peaks at 350 and 470 nm. Kottmann and Martin [36] reported that the SPR peak at 350 nm corresponds to the out-of-plane quadrupole resonances originating from the Ag nanoparticles with tetrahedral shapes. This was confirmed by our XRD analyses which showed that the Ag nanoparticles prepared in this study were in the FCC phase (see Fig. 4). The TEM micrograph shown in Fig. 9(a), in which the Ag nanoparticles in tetrahedral form can be seen, also confirmed that the Ag nanoparticles prepared in this study were in the FCC structure. Widoniak *et al.* [37] reported that large particles with nonuniform shapes possess an extinction band at about 300 nm and that particles with sizes above 500 nm have no characteristic peaks at the wavelengths greater than 350 nm. As shown in Fig. 11, the results we obtained with the UV-visible spectrum of the sample prepared by using PVP with an  $M_w$  of 10 000 was in good agreement with Widoniak *et al.*'s results.

#### D. Effects of Reaction Time

Fig. 12 shows the TEM micrograph of Ag nanoparticles prepared at 120 °C for 24 h using tripropylene glycol as the reducing agent and 10 wt.% of PVP with an  $M_w$  of 55 000. Comparing with the Ag nanoparticles prepared at the same reaction conditions but different reaction times of 24 and 3 h, Fig. 9(a) shows that the prolonged reaction time, in fact, has little effect on aver-

age particle sizes, but the production yield of Ag nanoparticles increased from 50% to 80%. Furthermore, Fig. 12 indicates that the size and shape of Ag particles became nonuniform when the reaction time is increased. Phase transformation can be divided into four stages, i.e., the incubation period, steady-state nucleation, growth, and coarsening. As the reaction time increased, nucleation and growth exhausted the available  $\text{Ag}^+$  ions, and the coarsening of particles became the dominant process. The nonuniform particle size likely resulted from the Ostwald ripening effect or, the reduction of the surface energy, of the whole system. The theory of particle coarsening delineates that a chemical potential gradient will be built up in between the particles of different sizes. Small particles possess high surface curvature and, thus, high chemical potential, leading to a mass flow toward the large particles with low surface curvature. Large Ag particles coarsen at the expense of small Ag particles and, as the particles grow, they are enclosed preferentially by low-energy crystal planes, e.g., the  $\{1\ 1\ 1\}$  planes of FCC system, thereby reducing the total surface energy of sample. This results in Ag nanoparticles with tetrahedral and truncated octahedral shapes, as shown in Fig. 12.

#### IV. CONCLUSION

This paper presents the preparation of Ag nanoparticles *via* the polyol process by using tripropylene glycol, 3-ethyl-3-oxetanemethanol, or polycaprolactone triol as the reducing agent and PVP as the protecting agent. Tripropylene glycol was found to possess the highest reactivity due to its long-chain structure with abundant  $-\text{OH}$  groups that may efficiently initiate the reduction reaction. Tripropylene glycol combined with 20 wt.% of PVP with an  $M_w$  of 55 000 exhibited the best result, i.e., uniform Ag nanoparticles with an average size as small as 34.4 nm were produced at the reaction temperature of 120 °C for 3 h. In addition, these small Ag nanoparticles were produced with a shorter reaction time than the reaction times in previous studies that used EG as the reducing agent at the same reaction temperature of 120 °C. A shoulder peak appeared at 350 nm in the UV-visible spectrum, indicating that the synthesized Ag nanoparticles had an FCC structure. These results also were confirmed by TEM/EDS and XRD analyses. The morphology of the Ag nanoparticles was characterized by TEM which indicated that the size and shape of the Ag nanoparticles were affected by the  $M_w$  value and the concentration of PVP used for the reduction reaction.

#### REFERENCES

- [1] J. Perelaer, B. de Gans, and U. S. Schubert, "Ink-jet printing and microwave sintering of conductive silver tracks," *Adv. Mater.*, vol. 18, no. 16, pp. 2101–2104, Aug. 2006.
- [2] A. L. Dearden, P. J. Smith, D.-Y. Shin, N. Reis, B. Derby, and P. O'Brien, "A low curing temperature silver ink for use in ink-jet printing and subsequent production of conductive tracks," *Macromol. Rapid Commun.*, vol. 26, no. 4, pp. 315–318, Feb. 2005.
- [3] Z. Liu, Y. Su, and K. Varshneyan, "Inkjet-printed silver conductors using silver nitrate ink and their electrical contacts with conducting polymers," *Thin Solid Films*, vol. 478, no. 1–2, pp. 275–279, May 2005.
- [4] E. Nisaratanaporn and K. Wongsuwan, "Preparation of ultrafine silver powder using glycerol as reducing agent," *J. Met. Mater. Miner. Soc.*, vol. 18, no. 2, pp. 1–5, 2008.



- [5] Z. Zhang, B. Zhao, and L. Hu, "PVP protective mechanism of ultrafine silver powder synthesized by chemical reduction processes," *J. Solid State Chem.*, vol. 121, no. 1, pp. 105–110, Jan. 1996.
- [6] K. S. Chou and C. Y. Ren, "Synthesis of nanosized silver particles by chemical reduction method," *Mater. Chem. Phys.*, vol. 64, no. 3, pp. 241–246, May 2000.
- [7] Y. Zhu, Y. Qian, M. Zhang, and Z. Chen, "Preparation of nanocrystalline silver powders by  $\gamma$ -ray radiation combined with hydrothermal treatment," *Mater. Lett.*, vol. 17, no. 5, pp. 314–318, Sep. 1993.
- [8] H. S. Zhou, T. Wada, H. Sasabe, and H. Komiyama, "Synthesis of nanometer-size silver coated polymerized diacetylene composite particles," *Appl. Phys. Lett.*, vol. 68, no. 9, pp. 1288–1290, Feb. 1996.
- [9] K. Okitsu, H. Bandow, and Y. Maeda, "Sonochemical preparation of ultrafine palladium particles," *Chem. Mater.*, vol. 8, no. 2, pp. 315–320, Feb. 1996.
- [10] P. Y. Silvert, R. Herrera-Urbina, N. Duvauchelle, and V. Vijayakrishnan, "Preparation of colloidal silver dispersions by the polyol process," *J. Mater. Chem.*, vol. 6, no. 4, pp. 573–577, Apr. 1996.
- [11] F. Fievet, J. P. Lagier, and M. Figlarz, "Preparing monodisperse metal powders in micrometer and submicrometer sizes by the polyol process," *MRS Bull.*, vol. 24, no. 12, pp. 29–34, Dec. 1989.
- [12] A. Slistan-Grijalva, R. Herrera-Urbina, J. F. Rivas-Silva, M. Ávalos-Borja, F. F. Castellón-Barraza, and A. Posada-Amarillas, "Assessment of growth of silver nanoparticles synthesis from an ethylene glycol-silver nitrate-polyvinylpyrrolidone," *Physica E*, vol. 25, no. 4, pp. 438–448, Jan. 2005.
- [13] J. Bregado-Gutiérrez, A. J. Saldívar-García, and H. F. López, "Synthesis of silver nanocrystals by a modified polyol method," *J. Appl. Polym. Sci.*, vol. 107, no. 1, pp. 45–53, Jan. 2008.
- [14] Y. Gao, P. Jiang, L. Song, L. Liu, X. Yan, Z. Zhou, D. Liu, J. Wang, H. Uuan, Z. Zhang, X. Zhao, X. Dou, W. Zhou, G. Wang, and S. Xie, "Growth mechanism of silver nanowires synthesized by polyvinylpyrrolidone-assisted polyol reduction," *J. Phys. D: Appl. Phys.*, vol. 38, no. 7, pp. 1061–1067, 2005.
- [15] G. H. Jiang, L. Wang, T. Chen, H. J. Yu, and J. J. Wang, "Preparation and characterization of dendritic silver nanoparticles," *J. Mater. Sci.*, vol. 40, no. 7, pp. 1681–1683, Apr. 2005.
- [16] T. Maiyalagan, "Synthesis, characterization and electrocatalytic activity of silver nanorods towards the reduction of benzyl chloride," *Appl. Catal. A-Gen.*, vol. 340, no. 2, pp. 191–195, Jun. 2008.
- [17] P. Y. Silvert, H. R. Errera-Urbina, and K. Tekaiia-Elhsissen, "Preparation of colloidal silver dispersions by the polyol process. Part 2. Mechanism of particle formation," *J. Mater. Chem.*, vol. 7, no. 2, pp. 293–299, Feb. 1997.
- [18] K. H. Park, S. H. Im, and O. O. Park, "The size control of silver nanocrystals with different polyols and its application to low-reflection coating materials," *Nanotechnology*, vol. 22, no. 4, pp. 045602-1–045602-6, Jan. 2011.
- [19] B. He, J. J. Tan, K. Y. Liew, and H. Liu, "Synthesis of size controlled Ag nanoparticles," *J. Mol. Catal. A-Chem.*, vol. 221, no. 1/2, pp. 121–126, Dec. 2004.
- [20] D. Radziuk, A. Skirtach, G. Sukhorukov, D. Shchukin, and H. Möhwald, "Stabilization of silver nanoparticles by polyelectrolytes and polyethylene glycol," *Macromol. Rapid Commun.*, vol. 28, no. 7, pp. 848–855, Apr. 2007.
- [21] D. H. Chen and Y. W. Huang, "Spontaneous formation of Ag nanoparticles in dimethylacetamide solution of poly(ethylene glycol)," *J. Colloid Interface Sci.*, vol. 255, no. 2, pp. 299–302, Nov. 2002.
- [22] C. Luo, Y. Zhang, X. Zeng, Y. Zeng, and Y. Wang, "The role of poly(ethylene glycol) in the formation of silver nanoparticles," *J. Colloid Interface Sci.*, vol. 288, no. 2, pp. 444–448, Aug. 2005.
- [23] A. Sinha and B. P. Sharma, "Preparation of silver powder through glycerol process," *Bull. Mater. Sci.*, vol. 28, no. 3, pp. 213–217, Jun. 2005.
- [24] S. E. Skrabalak, B. J. Wiley, M. Kim, E. V. Formo, and Y. Xia, "On the polyol synthesis of silver nanostructures: Glycolaldehyde as a reducing agent," *Nano Lett.*, vol. 8, no. 7, pp. 2077–2081, Jun. 2008.
- [25] M. Darroudi, M. B. Ahmad, A. H. Abdullah, and N. A. Ibrahim, "Green synthesis and characterization of gelatin-based and sugar-reduced silver nanoparticles," *Int. J. Nanomed.*, vol. 6, no. 1, pp. 569–574, 2011.
- [26] A. Šileikaitė, J. Puišo, I. Prosyčėvas, and S. Tamulevičius, "Investigation of silver nanoparticles formation kinetics during reduction of silver nitrate with sodium citrate," *Mater. Sci.*, vol. 15, no. 21, pp. 21–27, 2009.
- [27] M. M. Cook and J. A. Lander, "Use of sodium borohydride to control heavy metal discharge in the photographic industry," *J. Appl. Photogr. Eng.*, vol. 5, no. 3, pp. 144–147, 1979.
- [28] T. H. Chiang and T.-E. Hsieh, "A study of monomer's effect on adhesion strength of UV-curable resins," *Int. J. Adhesion Adhesives*, vol. 26, no. 4, pp. 520–531, Aug. 2006.
- [29] C. Ducamp-Sanguesa, R. Herrera-Urbina, and M. Figlarz, "Synthesis and characterization of fine and monodisperse silver particles of uniform shape," *J. Solid State Chem.*, vol. 100, no. 2, pp. 272–280, Oct. 1992.
- [30] P. K. Sahoo, S. S. Kalyan, K. Kamal, T. Jagadeesh, B. Sreedhar, A. K. Singh, and S. K. Srivastava, "Synthesis of silver nanoparticles using facile wet chemical route," *Def. Sci. J.*, vol. 59, no. 4, pp. 447–455, Jul. 2009.
- [31] W. Zhang, X. Qiao, and J. Chen, "Formation of silver nanoparticles in SDS inverse microemulsions," *Mater. Chem. Phys.*, vol. 109, no. 2–3, pp. 411–416, Jun. 2008.
- [32] S. L. Smitha, K. M. Nissamudeen, D. Philip, and K. G. Gopchandran, "Studies on surface plasmon resonance and photoluminescence of silver nanoparticles," *Spectrochim Acta A-Mol. Biomol. Spectrosc.*, vol. 71, no. 1, pp. 186–190, Nov. 2008.
- [33] Y. Zhao, Y. Jiang, and Y. Fang, "Spectroscopy property of Ag nanoparticles," *Spectrochim Acta A-Mol. Biomol. Spectrosc.*, vol. 65, no. 5, pp. 1003–1006, Dec. 2006.
- [34] O. A. Usov, A. I. Sidorov, A. V. Nashchekin, O. A. Podsvirov, N. V. Kurbatova, V. A. Tsekhomsky, and A. V. Vostokov, "SPR of Ag nanoparticles in a photochromic glasses," *Proc. SPIE*, vol. 7394, pp. 7394J-1–7394J-6, Aug. 2009.
- [35] B. Wiley, Y. Sun, B. Mayers, and Y. Xia, "Shape-controlled synthesis of metal nanostructures: The case of silver," *Chem. Eur. J.*, vol. 11, no. 2, pp. 454–463, Jan. 2005.
- [36] J. Kottmann and O. J. F. Martin, "Plasmon resonances of silver nanowires with a nonregular cross section," *Phys. Rev. B.*, vol. 64, no. 23, pp. 235402-1–235402-10, Nov. 2001.
- [37] J. Widoniak, S. Eiden-Assmann, and G. Maret, "Silver particles tailoring of shapes and sizes," *Colloid Surf. A-Physicochem. Eng. Aspects*, vol. 270–271, pp. 340–344, Dec. 2005.



**Tzu Hsuan Chiang** received the B.S. degree in chemical engineering from the National Taiwan University of Science and Technology, Taipei, Taiwan, in 1996, the M.S. degree in chemical and materials engineering from Chang Chung University, Taoyuan, Taiwan, in 2002, and the Ph.D. degree in materials science and engineering from National Chiao Tung University, Hsinchu, Taiwan, in 2006.

From 2006 to 2007 and 2007 to 2009, she was an Assistant Professor with the Environmental Engineering and Biotechnology Department, Chin Min Institute of Technology. Since November 2009, she has been an Assistant Professor with the Energy Engineering Department, National United University, Miaoli, Taiwan. Her research interests include polymer composites, UV-curable adhesives, and silver pastes.



**K.-D. Wu** received the B.S. degree in chemistry from the National Dong Hwa University, Hualien, Taiwan, in 2005, and the M.S. degree from the National Chiao Tung University, Hsinchu, Taiwan, in 2008, in Industrial Technology R&D Master Program on Materials and Processes of Semiconductor.

She is currently working as an Engineer at Taiwan Semiconductor Manufacturing Company, Ltd., Hsinchu, Taiwan.



**Tsung-Eong Hsieh** received the B.S. degree in physics from the National Taiwan Normal University, Taiwan, in 1979. He then transferred his major to materials science and engineering and received the M.S. degree from the National Tsing Hua University, Taiwan, in 1981 and the Ph.D. degree from Massachusetts Institute of Technology, Cambridge, MA, USA, in 1988.

He is currently a Faculty Member at the Department of Materials Science and Engineering, National Chiao Tung University, Hsinchu, Taiwan. His research interests include optoelectronic materials and devices, optical and electrical storage media, energy resource materials, electronic packaging, thin-film technology, and materials characterizations.